8-1-2010

Noise analysis for 3-point chemical shift-based water-fat separation with spectral modeling of fat

Venkata V. Chebrolu
University of Wisconsin-Madison

Huanzhou Yu
GE Healthcare, United States

Angel R. Pineda
California State University, Fullerton

Charles A. McKenzie
Western University, cmcken@uwo.ca

Jean H. Brittain
GE Healthcare, United States

See next page for additional authors

JOURNAL OF MAGNETIC RESONANCE IMAGING 32:493–500 (2010)

Technical Note

Noise Analysis for 3-Point Chemical Shift-Based Water-Fat Separation With Spectral Modeling of Fat

Venkata V. Chebrolu, MS,[1] Huanzhou Yu, PhD,[2] Angel R. Pineda, PhD,[3] Charles A. McKenzie, PhD,[4] Jean H. Brittain, PhD,[5] and Scott B. Reeder, MD, PhD[1,6–8]*

Purpose: To model the theoretical signal-to-noise ratio (SNR) behavior of 3-point chemical shift-based water-fat separation, using spectral modeling of fat, with experimental validation for spin-echo and gradient-echo imaging. The echo combination that achieves the best SNR performance for a given spectral model of fat was also investigated.

Materials and Methods: Cramér-Rao bound analysis was used to calculate the best possible SNR performance for a given echo combination. Experimental validation in a fat-water phantom was performed and compared with theory. In vivo scans were performed to compare fat separation with and with out spectral modeling of fat.

Results: Theoretical SNR calculations for methods that include spectral modeling of fat agree closely with experimental SNR measurements. Spectral modeling of fat more accurately separates fat and water signals, with only a slight decrease in the SNR performance of the water-only image, although with a relatively large decrease in the fat SNR performance.

Conclusion: The optimal echo combination that provides the best SNR performance for water using spectral modeling of fat is very similar to previous optimizations that modeled fat as a single peak. Therefore, the optimal echo spacing commonly used for single fat peak models is adequate for most applications that use spectral modeling of fat.

Key Words: chemical shift imaging; water-fat separation; IDEAL; spectral modeling of fat; Cramér-Rao bound
J. Magn. Reson. Imaging 2010;32:493–500.

CHEMICAL SHIFT-BASED water-fat separation methods have seen a recent increase in clinical use for suppressing fat signal. The high signal intensity of fat can obscure underlying pathology such as edema in T_2-weighted sequences and enhancing tissue in contrast-enhanced T_1-weighted imaging. Multipoint chemical shift-based water-fat separation methods (1–4) such as IDEAL (iterative decomposition of water and fat with echo asymmetry and least squares estimation) (5,6) are known to provide robust qualitative separation of water and fat signal with good signal-to-noise ratio (SNR) even in the presence of B_0 and B_1 field inhomogeneities, where conventional fat suppression methods are either inadequate or have reduced SNR performance (7,8).

Most chemical shift-based water-fat separation methods model fat as a single peak, separated ≈3.5 ppm (parts per million) from the water peak. Although water has a single discrete peak, fat has multiple peaks that arise from different chemical moieties (protons on different carbon chains) each with different chemical shifts (9,10). The presence of multiple fat peaks, if not modeled accurately, leads to incomplete separation of fat signal for qualitative fat suppression methods and confounds attempts at quantifying fat using quantitative approaches (9,11). For example, signal from olefinic proton, whose resonance frequency (5.3 ppm) is close to that of water's resonance frequency, will partly separate into the water signal. This signal appears as "gray fat" (7) in chemical shift-based water-fat separation methods and represents incompletely separated fat signal remaining in the water image. Moreover, for fat quantification, spectral modeling of fat is necessary to avoid large errors that may be clinically significant (12,13).

[1]Department of Biomedical Engineering, University of Wisconsin, Madison, Wisconsin, USA.
[2]Global MR Applied Science Laboratory, GE Healthcare, Menlo Park, California, USA.
[3]Department of Mathematics, California State University, Fullerton, California, USA.
[4]Department of Medical Biophysics, University of Western Ontario, London, Ontario, Canada.
[5]Global MR Applied Science Laboratory, GE Healthcare, Madison, Wisconsin, USA.
[6]Department of Radiology, University of Wisconsin, Madison, Wisconsin, USA.
[7]Department of Medical Physics, University of Wisconsin, Madison, Wisconsin, USA.
[8]Department of Medicine, University of Wisconsin, Madison, Wisconsin, USA.
Contract grant sponsor: National Institutes of Health (NIH); Contract grant number: RC1EB010384; Contract grant sponsor: GE Healthcare.
*Address reprint requests to: S.B.R., Department of Radiology, E3/311 CSC, University of Wisconsin, 600 Highland Ave., Madison, WI 53792-3252. E-mail: sreeder@wisc.edu
Received January 21, 2010; Accepted April 6, 2010.
DOI 10.1002/jmri.22220
Published online in Wiley InterScience (www.interscience.wiley.com).

The noise performance of 3-point water-fat separation methods that model fat as a single, discrete peak (single peak model) has previously been characterized theoretically (14) and experimentally (6). Using this model, SNR performance is maximized when the phase shift between water and fat signals are ($-\pi/6+\pi k$, $\pi/2+\pi k$, $7\pi/6+\pi k$), where k is any integer. The inclusion of multiple fat peaks in the signal model (multipeak model), however, changes the model and alters the noise performance of the separated water and fat signals. The purpose of this work is to ascertain the SNR behavior of chemical shift imaging including spectral modeling of fat and to provide experimental validation. For comparison of optimal echo times of multipeak and single peak models, we will refer to the phase difference between water and the main fat peak (peak with $\Delta f_p = -210$ Hz relative to water at 1.5T) as the phase between water and "fat."

THEORY

The signal from a voxel containing water and fat can be written as:

$$s(t) = \left(We^{i\phi_W} + Fe^{i\phi_F} \sum_{p=1}^{P} r_p e^{i2\pi\Delta f_p t} \right) e^{i2\pi\psi t} + \varepsilon \qquad [1]$$

where W and F are the magnitude of water and fat signals, ψ_W and ψ_F are the phase of water and fat signals at $t = 0$ sec (during radiofrequency [RF] excitation), Ψ is the local field inhomogeneity (Hz), Δf_p is frequency of the p^{th} fat peak and r_p are the relative amplitudes of the different fat peaks, such that $\sum_{p=1}^{P} r_p = 1$. It was assumed that all fat peaks had a common initial phase (ψ_F) based on the work of Yu et al (9). It is important to note that both frequencies (Δf_p) and relative amplitudes (r_p) of the fat peaks are also assumed to be known. The values of Δf_p and r_p can be measured with magnetic resonance spectroscopy (MRS) (12,15). The values of r_p can also be calculated using pre- or self-calibration methods (5,9). These methods were used to estimate the spectral content of fat in adipose tissue (9), peanut oil (9), liver (15), and other areas of clinical interest (9). The noise on the measured signal, ε, is assumed to be Gaussian with zero mean and uncorrelated at different times, t(16). Note that for this work the effects of T_2^* decay have been ignored, which is a reasonable assumption for short echo times and a small number of echoes (eg, three (6)) spaced closely in time.

A useful metric for the noise performance of a water-fat decomposition is the effective number of signal averages, or NSA (1,2,17), defined as:

$$NSA = \frac{\sigma^2}{\sigma_\rho^2} \qquad [2]$$

where σ^2 is the variance of the noise in a source image and σ_ρ^2 is the variance of the noise in a calculated water or fat image. The minimum value of σ_ρ^2 that can be achieved by an unbiased estimator was computed using Cramér-Rao Bound (CRB) analysis and compared with the values estimated using single peak and multipeak models.

The theoretical noise behavior of the water signal was computed to determine the optimum echo combination that provides the best SNR performance for water-fat separation with multipeak reconstruction using the CRB analysis. CRB analysis uses Fisher information matrix (FIM) (14,17) to estimate the sensitivity of data acquired to the parameters that are being estimated in the presence of noise.

If **S** is the vector representation of the data, and **P** is the vector representation of the parameters to be estimated (W, F, ψ_W, ψ_F, and Ψ) then the (k, l)$^{\text{th}}$ element of the FIM is given by the equation:

$$FIM_{kl} = \left\langle \frac{\partial}{\partial p_k} \frac{\partial}{\partial p_l} \ln \Pr(\mathbf{S}|\mathbf{P}) \right\rangle \qquad [3]$$

where Pr(**S**|**P**) is the probability of observing **S** given **P**. The theoretical minimum values for the variance of the estimates of W, F, ψ_W, ψ_F, and Ψ are given by the inequality:

$$\sigma_{\hat{p}_k}^2 \geq [FIM^{-1}]_{kk} \qquad [4]$$

where $\hat{p}_k$ is the k^{th} element of **P**. The expressions related to the computation of FIM are described below. For a group of three echoes measured at specific echo times, $t_n (n = 1, 2, 3)$, we can write Eq. [1] in a matrix format:

$$\mathbf{S} = \mathbf{A}\Gamma + \varepsilon \qquad [5]$$

where:

$$\mathbf{A}_{6x2} = \begin{bmatrix} \cos(\psi_W + 2\pi\psi t_1) & \sum_{p=1}^{P} r_p \cos(\psi_F + 2\pi\psi t_1 + 2\pi\Delta f_p t_1) \\ \sin(\psi_W + 2\pi\psi t_1) & \sum_{p=1}^{P} r_p \sin(\psi_F + 2\pi\psi t_1 + 2\pi\Delta f_p t_1) \\ \cos(\psi_W + 2\pi\psi t_2) & \sum_{p=1}^{P} r_p \cos(\psi_F + 2\pi\psi t_2 + 2\pi\Delta f_p t_2) \\ \sin(\psi_W + 2\pi\psi t_2) & \sum_{p=1}^{P} r_p \sin(\psi_F + 2\pi\psi t_2 + 2\pi\Delta f_p t_2) \\ \cos(\psi_W + 2\pi\psi t_3) & \sum_{p=1}^{P} r_p \cos(\psi_F + 2\pi\psi t_3 + 2\pi\Delta f_p t_3) \\ \sin(\psi_W + 2\pi\psi t_3) & \sum_{p=1}^{P} r_p \sin(\psi_F + 2\pi\psi t_3 + 2\pi\Delta f_p t_3) \end{bmatrix} \qquad [6]$$

$$\mathbf{S}_{6x1} = [s^r(t_1) \quad s^i(t_1) \quad s^r(t_2) \quad s^i(t_2) \quad s^r(t_3) \quad s^i(t_3)]^T \qquad [7]$$

$$\Gamma_{2x1} = [W \quad F]^T \qquad [8]$$

$$\varepsilon_{6x1} = [\varepsilon_1^r \quad \varepsilon_1^i \quad \varepsilon_2^r \quad \varepsilon_2^i \quad \varepsilon_3^r \quad \varepsilon_3^i]^T \qquad [9]$$

$s^r(t_n)$ and $s^i(t_n)$ are the real and imaginary parts of $s(t_n)$, the signal at the n^{th} echo. ε_n^y and ε_n^i are the real and imaginary parts of the noise at the n^{th} echo. Compared to the signal model used with single peak for fat spectrum, the second column of the matrix **A** has changed from a single exponential term ($e^{i2\pi\Delta f_i t_n}$) to a sum of weighted exponentials ($\sum_{p=1}^{P} r_p e^{i2\pi\Delta f_p t_n}$). Using the formulation of the matrix **A** in Eq. [6] and using

Eq. [3], all the elements of the FIM were computed. The minimum variance of the unbiased estimator for the parameters was computed from the inverse of FIM according to Eq. [4]. Then the theoretical NSA values for the magnitude of water and fat at different fat-fractions or fat-water ratios were obtained using Eq. [2]. These theoretical values at different amounts of fat and water were also used to determine the optimal echo shifts for methods using multipeak signal model.

MATERIALS AND METHODS

Theoretical Maximum NSA and the Optimum Echo Combination

Using the CRB formulation, the maximum NSA achievable and the corresponding optimum echo combination for multipeak reconstruction were determined. For a particular echo combination, NSA values were computed for all possible fat-fractions (0 to 100% fat) for both the single and multipeak models. The minimum NSA over all fat-water ratios (ie, worst case) was determined for each echo combination. The process of computing the minimum NSA was repeated for a large set of echo combinations. Finally, the echo combination that has the highest value for the "worst-case NSA" is chosen as the optimum echo combination because that echo combination gives the best possible SNR performance over all possible fat-fractions.

For many acquisitions, particularly multiple echo readouts, it is practical to maintain uniform echo spacing between adjacent echoes. Therefore, simulations (Fig. 1) were also performed for uniform echo spacing between adjacent echoes. The results of this computation comprise a subset of the earlier computation where echo spacing was allowed to vary independently between adjacent echoes.

Phantom Imaging

A spherical phantom with peanut oil floating on 0.9% normal saline doped with 5 mM $NiCl_2$ to shorten the T_1 was used for all SNR experiments. Even though the spectrum of triglycerides in human tissue (9,12) and that of peanut oil (9) are slightly different, the effect of the presence of multiple fat peaks on the NSA performance can be demonstrated using this phantom.

Imaging of the phantom was performed with modified 2D fast spin-echo (FSE) and 2D spoiled gradient-echo (SPGR) pulse sequences at 1.5T (Signa HDx TwinSpeed, GE Healthcare, Waukesha, WI), using an acquisition slab obliquely oriented across the fat-water interface to achieve a wide range of fat-fractions (Fig. 2). Both symmetric ($-2\pi/3,0,2\pi/3$, ie, TE = −1.58, 0, −1.58 ms) and asymmetric ($-\pi/6,\pi/2,7\pi/6$, ie, TE = −0.39, 1.19, 2.77 ms) echo spacings were chosen. The asymmetric combination has previously been shown to provide optimal SNR performance for single peak fat models. For SPGR imaging a phase shift of 0 is not achievable, and so echo combinations of ($4\pi/3,2\pi,8\pi/3$, ie, TE = 3.18, 4.76, 6.35 ms) and ($5\pi/6,3\pi/2,13\pi/6$, ie, TE = 1.98, 3.57, 5.16 ms), were chosen as symmetric and the asymmetric echo combinations.

Each oblique image was repeated 200 times in order to measure noise performance on a pixel-by-pixel basis, as previously described (5,6).

A single channel extremity coil was used for all phantom imaging. For FSE the following image parameters were used: TR/TE_{eff} = 700/13.1 ms, 256 × 256 matrix, 1 signal average, 20 cm field of view (FOV), 9 mm slice, 16 echo train length, and ±31.3 kHz bandwidth (scan time = 2:05 hours). For SPGR, the following imaging parameters were used: TR/TE = 10.0/(3.18,4.76,6.35) ms for symmetric echoes, TR/TE = 10.0/(1.98,3.57,5.16) ms for asymmetric echoes, 256 × 256 matrix, 1 signal average, 24 cm FOV, 10 mm slice, ±83.3 kHz bandwidth, and 50° flip angle (scan time = 25 min).

Volunteer scans were performed on GE 3.0T VH/i (HDx, GE Healthcare) magnetic resonance imaging (MRI) system with informed consent, approval of our Institutional Review Boards and in compliance with Health Insurance Portability and Accountability Act (HIPAA) regulations. An 8-channel neurovascular coil (GE Healthcare) was used for imaging the brachial plexus. Imaging parameters included: FSE imaging, TR/TE_{eff} = 2900/28.5 ms, 288 × 192 matrix, 2 signal averages, 30 cm FOV, 3 mm slice, 11 echo train length, and ±62.5 kHz bandwidth (scan time = 5:31 min). An 8-channel extremity coil (GE Healthcare) was used for imaging the knee. Imaging parameters include: SPGR imaging, TR/TE = 12.5/(4.56,5.35,6.15) ms, 384 × 224 matrix, 1 signal average with partial k_y acquisition (0.80), and homodyne reconstruction (18), 15 cm FOV, 1.0 mm slice, ±31.25 kHz bandwidth, and flip angle = 50° (43 slices, scan time = 4:55 min).

Images were reconstructed online using an investigational version of the multipeak (MP)-IDEAL and single peak (SP)-IDEAL reconstruction algorithms. No field map (Ψ) smoothing (19) was performed for phantom experiments with either SP or MP models, for both FSE and SPGR phantom experiments. Noise variances from the water images and individual source images at the three echo times were computed on a pixel-by-pixel basis over the 200 images in order to measure NSA for each pixel (Eq. [2]). The fat-water ratio was calculated for each pixel by averaging all 200 separated water images and fat images to obtain very high SNR estimates of fat and water, and thus fat-water ratio. For each experiment NSA measurements were plotted against the fat-water ratio for all pixels.

RESULTS

The theoretical NSA calculations for the multipeak reconstruction predict a optimal echo combination for water/fat to be (-0.17π, 0.49π, 1.18π) for spin-echo and (0.86π, 1.51π, 2.19π) for gradient-echo, when using the spectral model corresponding to liver fat (15). Using these optimal echo combinations the SNR performance achieves an optimized value of the minimum NSA of ≈3.00 for water for both spin-echo and

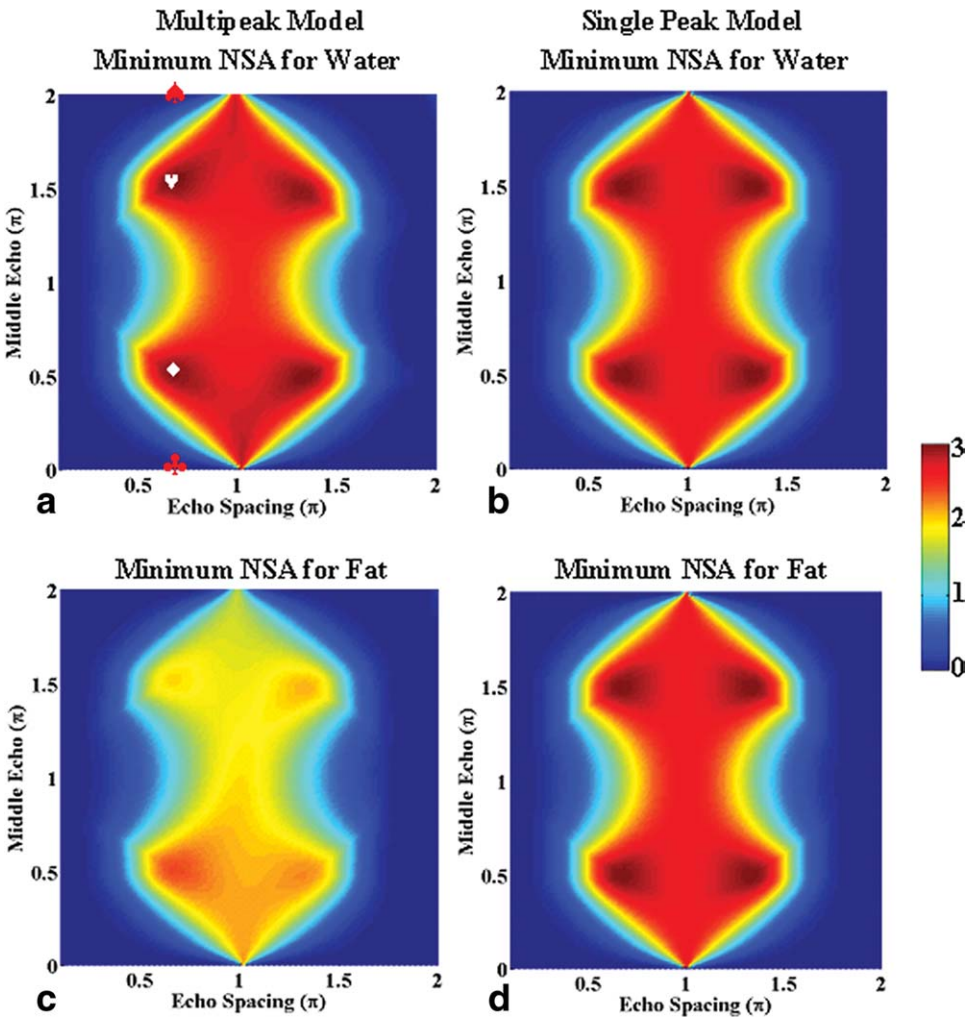

Figure 1. Theoretical minimum NSA for all possible fat-fractions (0 to 100% fat), calculated against middle echo and echo spacing for (**a**) water and (**c**) fat, computed using a spectral model of fat (15), and compared with minimum NSA for (**b**) water and (**d**) fat computed using the single peak model. ◆ and ♥ indicate the optimal echo combinations for SE and GRE, respectively. ♣ and ♠ indicate the nonoptimal symmetric echo combinations for SE (middle echo at 0) and GRE (middle echo at 2π), respectively, with "worst case" NSA of 0. The presence of multiple fat peaks significantly changes the NSA performance for fat (c), with only slight variation in the NSA performance for water (a). Therefore, the optimal echo spacing commonly used for single fat peak models is adequate for multipeak models when water-only image is the image of interest.

gradient-echo. However, the NSA for fat is ≈2.41 for spin-echo and ≈1.98 for gradient-echo, decreased from the maximum possible of 3.0 when using a single-peak model.

By comparison, the optimum SNR performance of the single peak model is achieved using the echo combinations (-0.17π, 0.50π, 1.17π) for spin-echo and (0.83π, 1.50π, 2.16π) for gradient-echo ($k = 1$), which correspond to the optimum echo combination for the single peak model, are very close to the optimum values for the multipeak model. Using the optimized echo combination of single peak model for multipeak reconstruction, a minimum NSA of ≈2.95 for water and ≈2.40 for fat can be obtained with spin-echo and a minimum NSA of ≈2.95 for water and ≈1.97 for fat with gradient-echo, theoretically. These computations repeated with the spectral models of fat in adipose tissue (9) and peanut oil (9) showed almost no difference in the optimal echo-combinations and "worst-case" NSA.

Figure 1 shows the theoretical minimum NSA for water (Fig. 1a,b) and fat (Fig. 1c,d) for all possible fat-fractions (0 to 100% fat), plotted for the middle echo (TE_2) and echo spacing using multipeak (Fig. 1a,c) and single peak (Fig. 1b,d) models. It can be observed that the optimum echo combinations for the multipeak model with a common echo spacing between adjacent echoes have similar middle echo values as that of single peak models for both water ($\pi/2$ and $3\pi/2$) and fat ($\pi/2$). Moreover, an echo spacing of 0.68π (Fig. 1a), which is only slightly greater than single peak optimal echo spacing of $2\pi/3$ (Fig. 1a), gives the

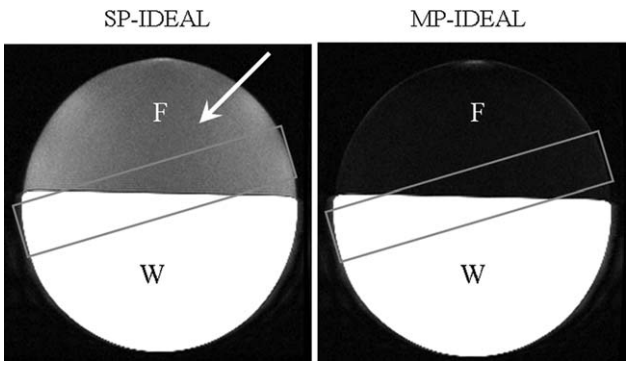

Figure 2. Improved fat-water separation can be seen by comparing the water images of oil-water phantom (axial) reconstructed with (left) SP-IDEAL and (right) MP-IDEAL both imaged using spin echo pulse sequence. Residual fat signal (shown with arrows in SP) in the water image of the single peak reconstruction is partially caused by fat peaks near the water peak. Window/levels are the same. W = water, F = fat.

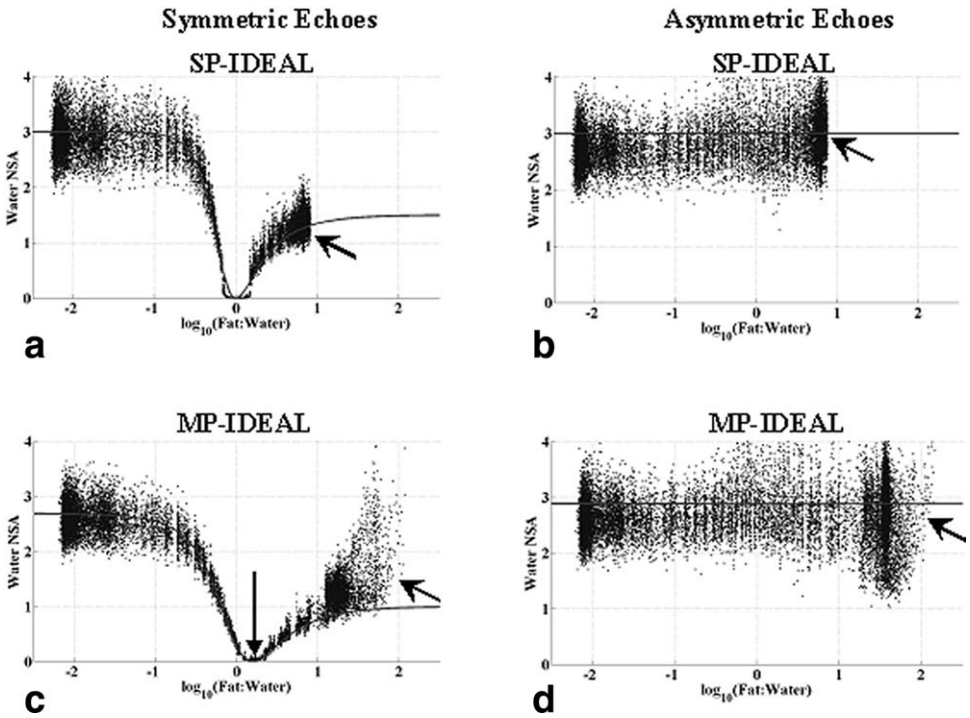

Figure 3. Theoretical and experimental NSA of water for (**a,b**) single peak and (**c,d**) multipeak signal models, imaged using FSE, with (a,c) symmetric ($-2\pi/3,0,2\pi/3$) and (b,d) asymmetric echoes ($-\pi/6,\pi/2,7\pi/6$) echoes. Dots are data and lines are theoretical predictions. NSA for (a) single peak model with symmetric echoes show poor noise performance (NSA = 0) when water and fat are in same proportions within a voxel (ie, fat-water ratio = 1) (6,14). Similar poor noise performance (long arrow) is observed, however, at a fat-water ratio slightly greater than 1 with MP-IDEAL due to spectral modeling of fat. Maximum achievable fat-water ratio (short arrows) increased 10 times with MP-IDEAL reconstruction, indicating greatly improved separation of water and fat signals provided by spectral modeling of fat. Close agreement between theory and experiment was observed.

best noise performance for the multipeak model. Therefore, the optimal echo spacing commonly used for single fat peak models is adequate for multipeak reconstruction when the signal in the water-only image is of primary interest (ie, fat suppression).

Figure 2 shows axial scans through the oil-water phantom acquired using asymmetrically acquired echoes ($-\pi/6$, $\pi/2$, $7\pi/6$) reconstructed using single (SP) and multipeak (MP) signal models. Improved separation of water and fat is achieved with the multipeak reconstruction because of a more accurate modeling of the fat spectrum. "Gray" fat seen on the single peak model reconstruction images represents residual fat signal that was incompletely separated.

Theoretical and experimental NSA performance of the calculated water image of oil-water phantom for single peak and multipeak models with both symmetric echoes ($-2\pi/3,0,2\pi/3$) and asymmetric echoes ($-\pi/6,\pi/2,7\pi/6$) are shown in Fig. 3 for the FSE acquisition. Excellent agreement between theory and experiment is seen with both echo combinations and both reconstruction methods. Both SP-IDEAL and MP-IDEAL reconstructions achieve CRB predictions. NSA for (Fig. 3a) single peak model with symmetric echoes show poor noise performance (NSA = 0) when water and fat are in same proportions within a voxel (ie, fat-water ratio = 1) (6,14). The nadir where NSA = 0 occurs at a fat-water ratio slightly greater than 1 (Fig. 3c) with MP-IDEAL. Importantly, the maximum noise performance for water is only slightly decreased (less than 10%) when using the multipeak reconstruction method. This indicates that the optimized asymmetric echo combinations for single peak reconstruction also perform well for multipeak reconstruction. Moreover, multipeak reconstruction results in increased range of fat-water ratios seen in Fig. 3b,d, where the maximum fat-water ratio increases from $\approx$10 to $\approx$100. The maximum apparent fat-water ratio was artifactually low because some of the fat signal incorrectly was assigned as water when using a single peak model.

Figure 4 shows NSA performance of the calculated water image of the oil-water phantom for single peak and multipeak models with SPGR sequence for both symmetric echoes ($4\pi/3,2\pi,8\pi/3$) and asymmetric echoes ($5\pi/6,3\pi/2,13\pi/6$). Improved agreement between theory and experiment, and improved separation of water and fat can be observed with spectral modeling of fat. For SPGR the echo times are longer and not including T_2* decay into the signal model may have resulted in this small deviation of experimental results from theoretical prediction of NSA, as seen at fat-water ratios close to 1.

Figure 5 shows the water images from a coronal brachial plexus (Fig. 5a,b) FSE scan and from a sagittal knee (Fig. 5c,d) SPGR scan, reconstructed using single (Fig. 5a,c) and multipeak (Fig. 5b,d) signal models. Subcutaneous fat is visibly better separated

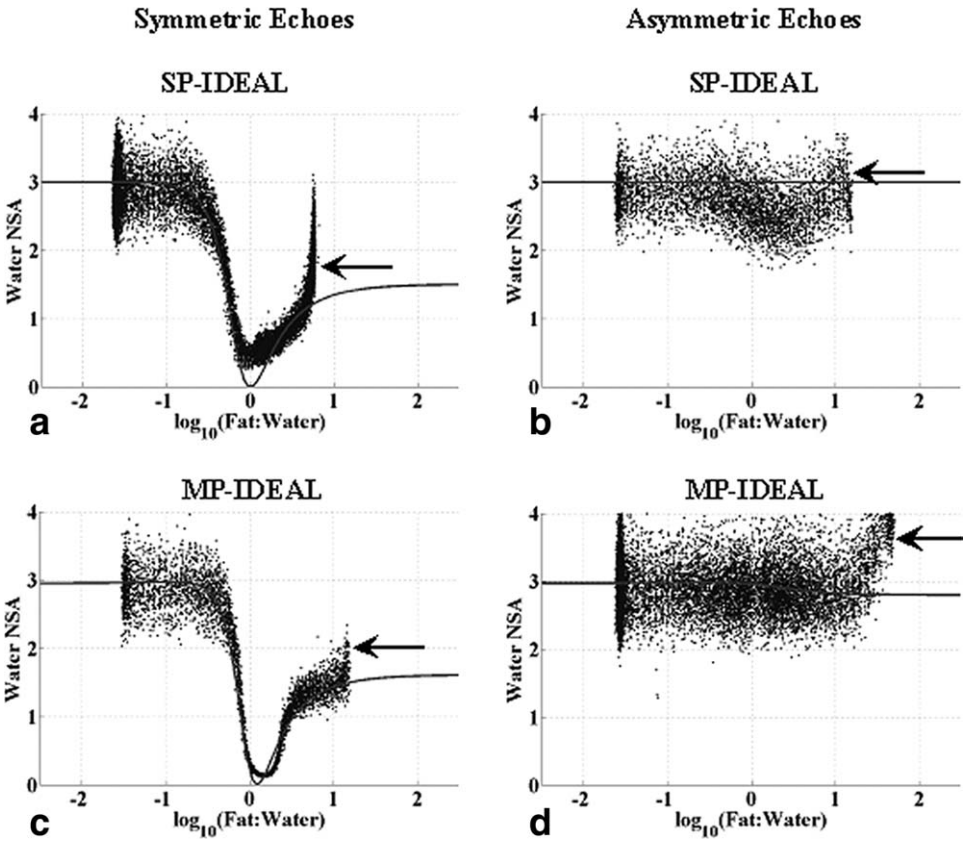

Figure 4. Theoretical and experimental NSA of water for (**a,b**) single peak and (**c,d**) multipeak signal models, imaged using SPGR, with symmetric echoes ($4\pi/3,2\pi,8\pi/3$) and asymmetric echoes ($5\pi/6,3\pi/2,13\pi/6$). Dots are data and lines are theoretical predictions. Maximum achievable fat-water ratios (shown with arrows) increased with MP-IDEAL reconstruction. Close agreement between theory and experiment was observed with spectral modeling of fat.

from the water image reconstructed with spectral modeling of fat.

DISCUSSION

The use of multipeak spectral modeling of fat greatly improves fat-water separation by more accurately modeling the NMR spectrum of fat. This leads to improved suppression of "gray" fat and is also important for quantitative methods that measure fat concentration. However, such modeling alters the noise performance of water-fat decomposition, as demonstrated above both theoretically and experimentally. Interestingly, the optimal echo spacing for the three-echo single peak model also provides excellent noise performance for water reconstructed with spectral modeling of fat.

The SNR performance of the estimated fat signal, however, does decline significantly (best "worst-case NSA" of 2.40 and 1.97 for FSE and GRE, respectively) when fat is modeled with multiple peaks as compared to when fat is modeled as a single peak (best "worst-case NSA" of 3.0 for FSE and GRE). This behavior will have little impact for qualitative methods aimed at improved fat suppression, ie, only the water signal is of interest, but may become important for quantitative applications that use both the water and fat signals for estimation of fat-fraction. Experiments also demonstrated that the maximum achievable estimated fat-water ratios increased, because the fat peak at 5.3 ppm and the other fat peaks not considered in the single peak model are now correctly assigned.

In this work the Cramér-Rao bound was used to analyze the noise performance because it provides more quantitative information than the information provided by other metrics such as the condition number. The condition number provides an indication of the combined sensitivity of the estimated set of parameters to changes in the measured values. In this way the overall sensitivity to noise, and hence noise performance, can be evaluated. However, the condition number does not provide information about the specific variance of the individual estimated parameter (eg, water or fat). The Cramér-Rao bound, however, gives more specific information by providing the least possible variance of the individual estimated parameters and, therefore, is a more comprehensive means of evaluating the theoretical noise performance of the estimation problem.

Accurate spectral modeling of fat, while it avoids large estimation biases that occur with single peak models, will necessarily suffer from an unavoidable reduction in SNR performance for the fat-only image. This occurs because estimation of the signal in the fat peaks that lie near the water peak (eg, olefinic) are almost entirely dependent on the ability to resolve the signal in the main fat peaks, distant from the water peak. In this way we are trading reduction in estimation bias for reduction in noise performance. However, the adipose tissue in the water-only image still has an NSA close to three. Therefore, the drop of NSA in the fat image does not affect the contrast-to-noise ratio (CNR) between the tissues in the water image, and hence better separation of fat from the water image improves the CNR in the water image.

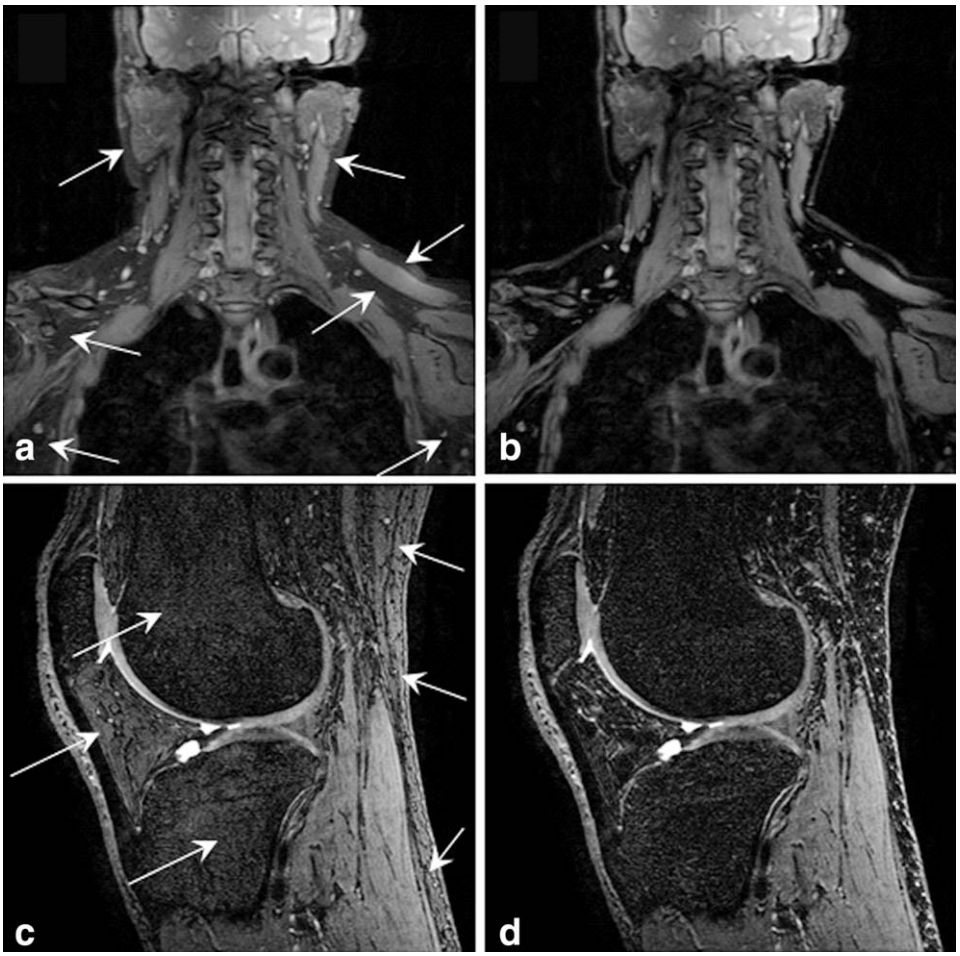

Figure 5. Improved separation of the subcutaneous fat can be seen by comparing the calculated water images of (**a,b**) brachial plexus and (**c,d**) knee, calculated with (a,c) SP-IDEAL and (b,d) MP-IDEAL reconstruction methods, imaged with spin-echo (a,b) and (c,d) gradient-echo imaging (c,d). Residual fat signal (shown with arrows in a,c) in the water image of the single peak reconstruction is due to bias from inaccurate modeling of fat (single peak).

An important assumption of the multipeak reconstruction approach used in this work is that the spectral model of fat is considered known. However, different types of fat may have different relative amplitudes of some of the various fat peaks. In vivo, however, the possible changes in these peaks are small. For example, the UCSD group (20) has shown in a large group of patients (>100) that the spectral characteristics of liver triglycerides are very similar with relatively small differences across patients. In addition, Cui et al (21) demonstrated 13% changes in the amplitude of the olefinic peak of triglycerides in adipose tissue with dramatic changes in the dietary intake of saturated vs. polyunsaturated fat. A 13% change in the olefinic peak, which carries ≈5% of the fat signal, would result in an ≈0.5% error for a voxel containing pure triglyceride, and a smaller error when fat is mixed with water. This represents a relatively small bias, particularly for qualitative applications.

In conclusion, this work investigated the use of the Cramér-Rao bound to analyze the noise performance of chemical shift-based water-fat separation methods that use spectral modeling of fat. The optimal echo combination that provides the best SNR performance for water using spectral modeling of fat is very similar to previous optimizations that modeled fat as a single peak. Therefore, the optimal echo spacing commonly used for single fat peak models is adequate for most applications that use spectral modeling of fat.

ACKNOWLEDGMENT

We thank the University of Wisconsin ICTR, funded through a National Institutes of Health (NIH) Clinical and Translational Science Award, number 1UL1RR025011.

REFERENCES

1. Glover GH. Multipoint Dixon technique for water and fat proton and susceptibility imaging. J Magn Reson Imaging 1991;1:521–530.
2. Xiang QS, An L. Water-fat imaging with direct phase encoding. J Magn Reson Imaging 1997;7:1002–1015.
3. Hernando D, Haldar JP, Sutton BP, Ma J, Kellman P, Liang ZP. Joint estimation of water/fat images and field inhomogeneity map. Magn Reson Med 2008;59:571–580.
4. Ma J. Breath-hold water and fat imaging using a dual-echo two-point Dixon technique with an efficient and robust phase-correction algorithm. Magn Reson Med 2004;52:415–419.
5. Yu H, McKenzie CA, Shimakawa A, et al. Multiecho reconstruction for simultaneous water-fat decomposition and T2* estimation. J Magn Reson Imaging 2007;26:1153–1161.
6. Reeder SB, Pineda AR, Wen Z, et al. Iterative decomposition of water and fat with echo asymmetry and least-squares estimation (IDEAL): application with fast spin-echo imaging. Magn Reson Med 2005;54:636–644.
7. Kijowski R, Woods MA, Lee KS, et al. Improved fat suppression using multipeak reconstruction for IDEAL chemical shift fat-water separation: application with fast spin echo imaging. J Magn Reson Imaging 2009;29:436–442.
8. Reeder SB, Yu H, Johnson JW, et al. T1- and T2-weighted fast spin-echo imaging of the brachial plexus and cervical spine with IDEAL water-fat separation. J Magn Reson Imaging 2006;24:825–832.

9. Yu H, Shimakawa A, McKenzie CA, Brodsky E, Brittain JH, Reeder SB. Multiecho water-fat separation and simultaneous R2* estimation with multifrequency fat spectrum modeling. Magn Reson Med 2008;60:1122–1134.
10. Reeder SB, Robson PM, Yu H, et al. Quantification of hepatic steatosis with MRI: the effects of accurate fat spectral modeling. J Magn Reson Imaging 2009;29:1332–1339.
11. Bydder M, Yokoo T, Hamilton G, et al. Relaxation effects in the quantification of fat using gradient echo imaging. Magn Reson Imaging 2008;26:347–359.
12. Yokoo T, Bydder M, Hamilton G, et al. Nonalcoholic fatty liver disease: diagnostic and fat-grading accuracy of low-flip-angle multiecho gradient-recalled-echo MR imaging at 1.5 T. Radiology 2009;251:67–76.
13. Szczepaniak LS, Nurenberg P, Leonard D, et al. Magnetic resonance spectroscopy to measure hepatic triglyceride content: prevalence of hepatic steatosis in the general population. Am J Physiol Endocrinol Metab 2005;288:E462–468.
14. Pineda AR, Reeder SB, Wen Z, Pelc NJ. Cramer-Rao bounds for three-point decomposition of water and fat. Magn Reson Med 2005;54:625–635.
15. Middleton MS, Hamilton G, Bydder M, Sirlin CB. How much fat is under the water peak in liver fat MR spectroscopy? In: Proc 17th Scientific Meeting ISMRM, Honolulu; 2009. p 4331.
16. McVeigh ER, Henkelman RM, Bronskill MJ. Noise and filtration in magnetic resonance imaging. Med Phys 1985;12:586–591.
17. Reeder SB, Wen Z, Yu H, et al. Multicoil Dixon chemical species separation with an iterative least-squares estimation method. Magn Reson Med 2004;51:35–45.
18. Reeder SB, Hargreaves BA, Yu H, Brittain JH. Homodyne reconstruction and IDEAL water-fat decomposition. Magn Reson Med 2005;54:586–593.
19. Yu H, Reeder SB, Shimakawa A, Brittain JH, Pelc NJ. Field map estimation with a region growing scheme for iterative 3-point water-fat decomposition. Magn Reson Med 2005;54:1032–1039.
20. Yokoo T, Bydder M, Hamilton G, et al. Effect of fat spectral model parameters on hepatic fat quantification by multi-echo gradient-echo magnetic resonance imaging. In: Proc 17th Scientific Meeting ISMRM, Honolulu; 2009. p 2134.
21. Cui M, Tomuta V, Segal-Isaacson C, Stein D, Hwang J. Abdominal fat measurement: MRS vs. MRI. In: Proc 16th Scientific Meeting ISMRM, Toronto; 2008. p 866.